Cooper Union for the Advancement of Science and Art

ChE 488 Final Project

Optimizing the Profit in Ethylene Production Via Thermal Cracking

Author:
Robert Brumer
Joshua Mayourian

Instructor:
Professor Davis

December 2013

Abstract

Hydrocarbon pyrolysis via thermal cracking produces ethylene, propylene, butadiene and aromatics, which are predominant feedstocks in the petrochemical industry. Our study optimizes the profit on the thermal cracking process of ethane to ethylene using a tubular reactor. Ethylene, ethane, and inert gases are fed into a tubular reactor at a temperature and pressure we can select. Furthermore, we can select the length, diameter, and constant wall temperature of the tubular reactor. We developed a model of the thermal cracking process based on this setup (Figure 1).

In this study, we assume that the inner diameter of the reactor is 0.1 m, which is approximately the inner diameter of a 4 inch schedule 80 stainless steel pipe. Furthermore, we require that the inlet inert and ethylene feed conditions are 30% of the total feed and 1 mol/s, respectively. We also requires that the single tubular reactor will fit in a 100 m by 1 m confined area. Therefore, the remaining decision variables are feed temperature, constant wall temperature, feed pressure, tube length, and ethane molar feed.

To solve this cost-optimization problem, we formulated a constrained, nonlinear programming problem. The optimal profit (neglecting capital cost) is $\$3.60/s$, which is equivalent to over $\$112,00,000$ per year, when the feed temperature, constant wall temperature, feed pressure, tube length, and ethane molar feed are 1050 ^{o}C, 1050 ^{o}C, 4.3 atm, 100 m, and 500 mol/s, respectively. This profit is much greater than the profit using previous conditions at our company, where we profited less than $\$22,00,000$ per year. A sensitivity analysis indicates that only by varying the parameters greatly will there be drastic change in our optimal solutions.

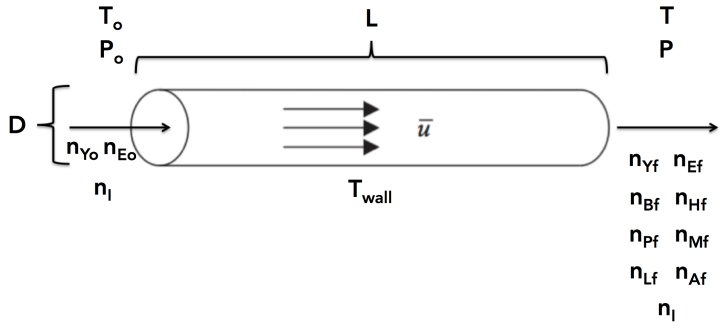

FIGURE 1: Schematic of Thermal Cracking of Ethane [1].

Table of Contents

List of Figures

List of Tables

Symbols

In order of appearance:

ΔG^o	standard Gibbs free energy	kJ/mol
ΔH^o	standard enthalpy	kJ/mol
T	temperature	K
ΔS^o	standard entropy	kJ/mol/K
$\overline{u}$	velocity	m/s
C_A	concentration of A	mol/m^3
z	length along reactor	m
R_A	reaction A	$mol/m^3/s$
N_A	molar flux of species A	$mol/m^2/s$
A_{pfr}	reactor cross-sectional area	m
n_A	molar rate of species A	mol/s
k_o	rate constant parameter	L/mol/s or 1/s
E	activation energy	kJ/mol
ΔH_R	heat of reaction	kJ
ρ	density	kg/m^3
C_p	specific heat	J/K
P	pressure	Pa
U	overall heat transfer coefficient	$J/m^2/K$
T_{ext}	reactor external temperature	K
Re	Reynolds number	unitless
n_{Yo}	inlet ethylene molar feed rate	mol/s
n_{Eo}	inlet ethane molar feed rate	mol/s
n_I	inlet inert molar feed rate	mol/s
T_o	inlet temperature	K
P_o	inlet pressure	Pa
L	tube length	m
D	tube inner diameter	m
T_{wall}	inner wall temperature	K

n_{Yf}	output ethylene molar rate	mol/s
n_{Ef}	output ethane molar rate	mol/s
n_{Bf}	output 1,3-butadiene molar rate	mol/s
n_{Pf}	output propane molar rate	mol/s
n_{Mf}	output methane molar rate	mol/s
n_{Lf}	output propylene molar rate	mol/s
n_{Af}	output acetylene molar rate	mol/s
k_1^f	forward rate constant of reaction 1	1/s
k_2	rate constant of reaction 2	1/s
k_5^f	forward rate constant of reaction 5	1/s
k_6	rate constant of reaction 6	L/mol/s
k_8	rate constant of reaction 8	L/mol/s
k_1^r	reverse rate constant of reaction 1	L/mol/s
k_5^r	reverse rate constant of reaction 5	L/mol/s
c_E	cost of ethane per mole	\$/mol
c_Y	cost of ethylene per mole	\$/mol
A	viscosity parameter 1	Pa $\cdot$ s /K^B
B	viscosity parameter 2	unitless
C	viscosity parameter 3	K
D	viscosity paramter 4	K^2
M	molecular weight	g/mol
μ	viscosity	Pa $\cdot$ s
k	thermal conductivity	W/m/K
v	velocity	m/s
$T_{o,min}$	minimum inlet temperature	K
$T_{wall,min}$	minimum wall temperature	K
$P_{o,min}$	minimum inlet pressure	Pa
$n_{Eo,min}$	minimum inlet ethane	mol/s
L_{min}	minimum length	m
$T_{o,max}$	maximum inlet temperature	K
$T_{wall,max}$	maximum wall temperature	K
$P_{o,max}$	maximum inlet pressure	Pa
$n_{Eo,max}$	maximum inlet ethane mole rate	mol/s
L_{max}	maximum length	m

Introduction

Chemical engineers frequently face problems that have multiple solutions, each with its own favorable and complicating economic and performance effects. Optimization techniques can be applied to avoid unsatisfactory economic and performance outcomes. Specifically, chemical engineers apply convex optimization techniques on process design, process synthesis, process operations, and process control models, which can be posed as linear programs (LPs), mixed integer linear programs (MILPs), quadratic programs (QPs), nonlinear programs (NLPs), or mixed integer nonlinear programs (MINLPs) [2]. In our study, we model and cost-optimize the thermal cracking process of ethane to ethylene using a tubular reactor.

1.1 Thermal Cracking Industrial Relevance

Hydrocarbon pyrolysis via thermal cracking produces ethylene, propylene, butadiene and aromatics, which are predominant feedstocks in the petrochemical industry [3]. The great desire to correctly model this reaction indicates the potential financial reward of this process [3–5]. Ethylene is a valuable product of this process with a $160 billion per year market alone [6]. Ethylene is produced more than any other organic compound due to its versatile chemical industrical use. Industrial uses of ethylene include polymerization, oxidation, halogenation, alkylation, hydration, oligomerization, and hydroformylation [7]. Therefore, in our study, we cost-optimized the thermal cracking of ethane to ethylene.

1.2 Background

Thermal Cracking

Vladimir Shukhov invented the first thermal cracking method in 1891 [8]. Thermal methods of hydrocarbon cracking involve reactions whose energetics are dominated mainly by the standard entropy term ΔS^o in the Gibbs free energy equation:

$$\Delta G^o = \Delta H^o - T\Delta S^o \tag{1.1}$$

where ΔG^o is the standard Gibbs free energy, T is the temperature, and ΔH^o is the standard enthalpy. In thermal cracking, the entropy term dominates the entropy term because of an extremely high temperature and the large increase in entropy from splitting a large molecule into smaller hydrocarbons. In our study, we apply the thermal cracking method to a non-isothermal tubular reactor.

Non-Isothermal Plug Flow Reactor

Chemical engineers commonly use a plug flow reactor to model thermal cracking. The concentration profile, temperature profile, and pressure profile within the tube can be modeled by using theoretically- and empirically-derived equations.

The governing mole balance equation for a non-isothermal plug flow reactor to find the concentration profile of species is:

$$\overline{u}\frac{dC_A}{dz} = R_A \tag{1.2}$$

where $\overline{u}$ is the velocity at a position z along the reactor, C_A is the concentration of species A, and R_a is the rate of reaction [1]. The governing energy balance equation for a non-isothermal plug flow reactor to find the temperature profile within the reactor is:

$$\frac{dT}{dz} = \frac{-\Delta H_R R}{\overline{u}\rho C_p} + \frac{1}{\rho C_p}\frac{dP}{dz} + \frac{2U}{\overline{u}\rho C_p R}(T_{ext} - T) \tag{1.3}$$

where ΔH_R is the enthalpy of reaction, ρ is the average density of the stream at location z, $\frac{dP}{dz}$ is the change in pressure along the reactor, C_p is the average specific heat, U is the overall heat transfer coefficient, R is the radius of the tube, and T_{ext} is the wall temperature [1]. The pressure drop within a non-bending plug flow reactor, which accounts for friction losses and changes in momentum, can be found from the equation [9, 10]:

$$\frac{dP}{dz} = \frac{\frac{d}{dz}(\frac{1}{M}) + \frac{1}{M}(\frac{1}{T}\frac{dT}{dz} + \frac{0.092\mathrm{Re}^{-0.2}}{D})}{\frac{1}{MP} - \frac{P}{\alpha\rho^2\overline{u}^2RT}} \tag{1.4}$$

where M is average molecular weight, Re is the Reynolds number, R is the gas constant, and α is the average convective heat transfer coefficient. We apply these basic principles in this study to model the thermal cracking of ethane to ethylene using a non-isothermal plug flow reactor. We obtained empirically-determined kinetic and physical parameters (viscosities, thermal conductivities, specific heats, and heats of formation) to accurately model this system [2, 3]. For more information on plug flow reactors and derivations of each of these governing equations, see Appendix A.

Problem Description and Methodology

2.1 Problem Statement

We seek to optimize the profit of the thermal cracking process shown below (Figure 2.1) using a plug flow reactor. Ethylene (Y), ethane (E), and inert (I) gases are fed into a plug flow reactor at molar flow rates labeled as n_{Yo}, n_{Eo}, and n_I in Figure 2.1, respectively. The inlet gases are fed into the reactor at temperature T_o and pressure P_o. The reactor has length L, diameter D, and constant inside wall temperature T_{wall}. In our study, we will use the reaction mechanism from Sundaram and Froment [3] (Figure 2.2) that demonstrates ethylene, ethane, 1,3-butadiene (B), hydrogen (H), propane (P), methane (M), propylene (L), acetylene (A), and inerts will be products of this process, at molar flow n_{Yf}, n_{Ef}, n_{Bf}, n_{Pf}, n_{Mf}, n_{Lf}, n_{Af}, and n_I in Figure 2.1, respectively.

We can select the inlet feed conditions (n_I, n_{Ei}, n_{Yi}, P_o, and T_o) and tube conditions (D, L, and T_{wall}). However, we will assume in this study that the inner diameter of the reactor is 0.1 m, which is approximately the inner diameter of a 4 inch schedule 80 stainless steel pipe [11]. Furthermore, we require that the inlet inert and ethylene feed conditions are 30% of the total feed and 1 mol/s, respectively. We also require that the single tubular reactor will fit in a 100 m by 1 m confined area. The remaining decision

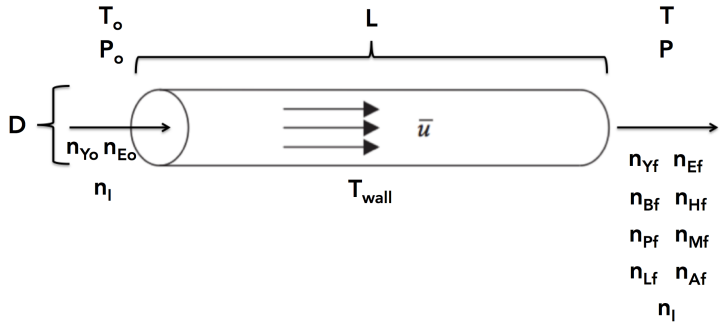

FIGURE 2.1: Schematic of Problem Statement[1].

$$C_2H_6 \underset{k_1^r}{\overset{k_1^f}{\rightleftarrows}} C_2H_4 + H_2$$

$$2C_2H_6 \xrightarrow{k_2} C_3H_8 + CH_4$$

$$C_3H_6 \underset{k_5^r}{\overset{k_5^f}{\rightleftarrows}} C_2H_2 + CH_4$$

$$C_2H_2 + C_2H_4 \xrightarrow{k_6} C_4H_6$$

$$C_2H_4 + C_2H_6 \xrightarrow{k_8} C_3H_6 + CH_4$$

FIGURE 2.2: Suggested Reaction Mechanism in This Study [3, 12]

variables are feed temperature, constant wall temperature, feed pressure, tube length, and ethane molar feed (Table 2.1).

TABLE 2.1: Decision Variables and Description

Decision Variables	Description
T_o	Feed Temperature (K)
T_{wall}	Constant Wall Temperature (K)
P_o	Feed Pressure (Pa)
L	Tube Length (m)
n_{Eo}	Ethane Molar Feed (mol/s)

2.2 Assumptions

Various justifiable assumptions are necessary for this cost-optimization study (in no particular order):

1. The costs of keeping the wall temperature T_{wall} constant, pumping the feed at pressure P_o, and feeding the reactants at temperature T_o are negligible compared to the profit from products produced.

2. Convection on the outside of the tube is rapid (the tube is within a furnace).

3. We are performing a retrofitting design on an existing furnace. The furnace cost is significantly greater than the additional capital cost. Therefore, we can neglect the annualized capital cost in our profit analysis.

4. The tube is constructed of stainless steel, and has a small enough thickness where the conduction resistance is negligible in the overall heat transfer coefficient.

5. The price of separating 1,3-butadiene, hydrogen, propane, methane, propylene, ethane, and acetylene is much greater than the sale price of these products such that they will likely just be burned as fuel. Therefore, the profit will be a function of the ethylene production and ethane feed.

6. There is negligible error in extrapolating viscosities outside of temperature range.

7. The mixture behaves as an ideal gas.

8. No mixing in the axial direction (no "back-mixing").

9. Rotational and radial symmetry for the concentration and velocity profiles.

10. $\frac{d}{dz}(\frac{1}{M})$ and $\frac{1}{MT}\frac{dT}{dz}$ are negligible and set equal to zero, which simplifies our pressure drop equation to:

$$\frac{dP}{dz} = \frac{\frac{1}{M}(\frac{0.092\mathrm{Re}^{-0.2}}{D})}{\frac{1}{MP} - \frac{P}{\alpha\rho^2\overline{u}^2RT}} \tag{2.1}$$

We found the pressure drop to be on the same magnitude as pressure drops in previous studies on this process, which justifies our assumptions.

2.3 Relevant Data

Seven types of parameters are necessary to fully describe this optimization problem:

1. Kinetic parameters for each reaction as a function of temperature
2. Viscosities of species as a function of temperature
3. Cost of each product and reactant
4. Thermal conductivity of species as a function of temperature
5. Specific heat of species as a function of temperature
6. Heats of formation of species
7. Molecular weight of species

The kinetic parameters are shown in Table 2.2.

TABLE 2.2: Kinetic Parameters for Each Reaction

Rate Constant	k_o (1/s or L/mol/s)	E_a (kcal/mol)	Reference
k_1^f	4.652×10^{13}	65.20	[3, 12]
k_2	3.850×10^{11}	65.25	[3, 12]
k_5^f	9.814×10^{8}	36.92	[3, 12]
k_6	1.026×10^{12}	41.26	[3, 12]
k_8	7.083×10^{13}	60.43	[3, 12]
k_1^r	8.75×10^{8}	32.69	[3, 12]
k_5^r	5.87×10^{4}	7.04	[3, 12]

The kinetic parameters for each reaction follow an Arrhenius-type model ($k = k_o e^{-E_a/RT}$). The viscosity of each species affects the Reynolds number and the pressure drop along the tube. The viscosity, μ is temperature dependent, where:

$$\mu(T) = \frac{AT^B}{1 + \frac{C}{T} + \frac{D}{T^2}} \tag{2.2}$$

Table 2.3 shows the parameters A, B, C, and D for each species.

TABLE 2.3: Viscosity of Species

Species	A	B	C	D	Reference
Ethane	2.5906×10^{-7}	0.67988	98.902	0	[13]
Ethylene	2.0789×10^{-6}	0.4163	352.7	0	[14]
Propane	4.9054×10^{-8}	0.90125	0	0	[15]
Propylene	7.3919×10^{-7}	0.5423	263.73	0	[16]
Acetylene	1.205×10^{-6}	0.4952	291.4	0	[17]
1,3-Butadiene	2.696×10^{-7}	0.6715	134.7	0	[18]
Hydrogen	1.797×10^{-7}	0.685	-0.59	140	[19]
Methane	5.2546×10^{-7}	0.59006	105.67	0	[20]
Water	1.7096×10^{-8}	1.1146	0	0	[21]

The profit objective function depends on the cost per mole of ethane and ethylene. The cost per mole of ethylene and ethane is shown in Table 2.4.

TABLE 2.4: Prices of Species

Species	Price ($/mol)	Reference
Ethane	$c_E = 0.0036$	[22]
Ethylene	$c_Y = 0.033$	[23]

The thermal conductivity appears in the energy balance on a differential element of a plug flow reactor. Therefore, the mean thermal conductivity affects the temperature profile along the reactor. The thermal conductivity, k, is temperature dependent, where:

$$k(T) = \frac{AT^B}{1 + \frac{C}{T} + \frac{D}{T^2}} \tag{2.3}$$

Table 2.5 shows the parameters A, B, C, and D for each species.

TABLE 2.5: Thermal Conductivity of Species

Species	A	B	C	D	Reference
Ethane	7.3869×10^{-5}	1.1689	500.73	0	[13]
Ethylene	8.6806×10^{-6}	1.4559	299.72	-2.9403×10^{4}	[14]
Propane	-1.1200	0.10972	-9834.6	-7.5358×10^{6}	[15]
Propylene	4.4900×10^{-5}	1.2018	421.00	0	[16]
Acetylene	7.5782×10^{-5}	1.0327	-36.227	3.1432×10^{4}	[17]
1,3-Butadiene	-2.0890×10^{4}	0.95930	-9.3820×10^{10}	0	[18]
Hydrogen	2.6530×10^{-3}	0.74520	12.000	0	[19]
Methane	8.3983×10^{-6}	1.4268	-49.654	0	[20]
Water	62.041×10^{-6}	1.3973	0	0	[21]

The specific heat also appears in the energy balance on a differential element of a plug flow reactor. Therefore, the mean specific heat affects the temperature profile along the reactor. Table 2.6 shows the specific heat parameters of each species. The specific heat, C_p, is temperature dependent, where:

$$C_p(T) = A + B\left(\frac{C}{Tsinh(\frac{C}{T})}\right)^2 + D\left(\frac{E}{Tcosh(\frac{E}{T})}\right)^2 \tag{2.4}$$

Table 2.6 shows the parameters A, B, C, and D for each species.

TABLE 2.6: Specific Heat of Species

Species	A	B	C	D	E	Reference
Ethane	44.256	84.737	872.24	67.130	2430.4	[13]
Ethylene	33.380	94.790	1596	55.100	740.8	[14]
Propane	59.474	12.661	844.31	86.165	2482.7	[15]
Propylene	43.852	15.060	1398.8	74.754	616.46	[16]
Acetylene	36.921	31.793	678.05	33.430	3036.6	[17]
1,3-Butadiene	50.950	17.050	1532.4	13.370	685.6	[18]
Hydrogen	7.617	9.560	2466	3.760	567.6	[19]
Methane	33.298	79.933	2086.9	41.602	991.96	[20]
Water	33.363	26.790	2610.5	8.896	1169	[21]

We must find the heat of reactions in this study for the temperature change. To do so, we need the heat of formation of each species. The heat of reactions contribute to the temperature profile as well. The heat of formation parameters of each species are shown in Table 2.7.

TABLE 2.7: Heat of Formation of Species

Species	Heat of Formation (kJ/mol)	Reference
Ethane	-83.82	[24]
Ethylene	52.51	[24]
Propane	-104.68	[24]
Propylene	20.23	[24]
Acetylene	228.2	[24]
1,3-Butadiene	109.24	[24]
Hydrogen	0	[24]
Methane	-74.52	[24]

Finally, we need the molecular weight of each species for varioius relations in our model. The molecular weight of each species is shown in Table 2.8.

TABLE 2.8: Molecular Weight of Species

Species	Molecular Weight (g/mol)	Reference
Ethane	30.07	[24]
Ethylene	28.054	[24]
Propane	44.096	[24]
Propylene	42.08	[24]
Acetylene	26.037	[24]
1,3-Butadiene	54.092	[24]
Hydrogen	2.016	[24]
Methane	16.042	[24]
Water	18.016	[24]

These kinetic and physical parameters allow us to accurately model our process. Our non-isothermal cracking model of ethane to ethylene is shown in the following section.

2.4 Non-Isothermal Cracking Model

Using the governing equations previously established and our assumptions, we state the differential equation equality constraints, the initial values for each differential equation, the algebraic equality constraints, and the decision variable inequality constraints in our model:

TABLE 2.9: Differential Equation and Initial Value Equality Constraints

Differential Variable	Differential Equation Equality Constraint	Initial Value Equality Constraint
N_E	$\frac{dN_E}{dz} = -k_1^f \frac{N_E}{\overline{u}} + k_1^r \frac{N_Y N_H}{\overline{u}^2} - 2k_2 \frac{N_E}{\overline{u}} - k_8 \frac{N_E N_Y}{\overline{u}^2}$	$N_E(z=0) = \frac{4n_{Eo}}{\pi D^2}$
N_Y	$\frac{dN_Y}{dz} = k_1^f \frac{N_E}{\overline{u}} - k_1^r \frac{N_Y N_H}{\overline{u}^2} - k_6 \frac{N_A N_Y}{\overline{u}^2} - k_8 \frac{N_E N_Y}{\overline{u}^2}$	$N_Y(z=0) = \frac{4n_{Yo}}{\pi D^2}$
N_H	$\frac{dN_H}{dz} = k_1^f \frac{N_E}{\overline{u}} - k_1^r \frac{N_Y N_H}{\overline{u}^2}$	$N_H(z=0) = 0$
N_P	$\frac{dN_P}{dz} = k_2 \frac{N_E}{\overline{u}}$	$N_P(z=0) = 0$
N_M	$\frac{dN_M}{dz} = k_2 \frac{N_E}{\overline{u}} + k_5^f \frac{N_L}{\overline{u}} - k_5^r \frac{N_M N_A}{\overline{u}^2} + k_8 \frac{N_E N_Y}{\overline{u}^2}$	$N_M(z=0) = 0$
N_L	$\frac{dN_L}{dz} = -k_5^f \frac{N_L}{\overline{u}} + k_5^r \frac{N_M N_A}{\overline{u}^2} + k_8 \frac{N_E N_Y}{\overline{u}^2}$	$N_L(z=0) = 0$
N_A	$\frac{dN_{Af}}{dz} = k_5^f \frac{N_L}{\overline{u}} - k_5^r \frac{N_M N_A}{\overline{u}^2} - k_6 \frac{N_A N_Y}{\overline{u}^2}$	$N_A(z=0) = 0$
N_B	$\frac{dN_{Bf}}{dz} = k_6 \frac{N_A N_Y}{\overline{u}^2}$	$N_B(z=0) = 0$
T	$\frac{dT}{dz} = \frac{-\Delta H_R R}{\overline{u}\rho C_p} + \frac{1}{\rho C_p}\frac{dP}{dz} + \frac{2U}{\overline{u}\rho C_p R}(T_{ext} - T)$	$T(z=0) = T_o$
P	$\frac{dP}{dz} = \frac{\frac{1}{M}(\frac{0.092\mathrm{Re}^{-0.2}}{D})}{\frac{1}{MP} - \frac{P}{\alpha\rho^2\overline{u}^2 RT}}$	$P(z=0) = P_o$

TABLE 2.10: Algebraic Equality Constraints

Algebraic Equality Constraints
$\mu = \sum_i \frac{\mu_i N_i}{N_i}$
$C_p = \sum_i \frac{C_{pi} N_i}{N_i}$
$M = \sum_i \frac{M_i N_i}{N_i}$
$k = \sum_i \frac{k_i N_i}{N_i}$
$\rho = \frac{PM}{RT}$
$\overline{u} = \frac{RT}{P}(\sum_i N_i)$
$Re = \frac{\rho \overline{u} D}{\mu}$
$k_z^f = k_{z,o} e^{-\frac{E_z}{R_z T}}$
$k_m^r = \frac{RT}{P} k_m^f e^{\frac{\Delta G_1}{RT}}$
$\mu_i(T) = \frac{A_i T^{B_i}}{1 + \frac{C_i}{T} + \frac{D_i}{T^2}}$
$\forall i = E, Y, H, P, M, L, A, B, I$
$\forall m = 1, 5$
$\forall z = 1, 2, 5, 6, 8$

The differential equation constraints can be solved with an ordinary differential equation solver, such as the Runge-Kutta-Fehlberg method. For more information on this algorithm, see Section 2.8.2.

The model of our thermal cracking process suggests our problem can be reduced to only five decision variables. This is because our equality constraints allow us remove many initial decision variables (N_L, N_A, N_B, etc.) where we only have to decide L, T_o, T_{wall}, n_{Eo}, and P_o.

2.5 Type of Optimization Problem

The problem statement (Section 2.1), assumptions (Section 2.2), available data (Tables 2.2 and 2.4), and model allows us to formally pose this cost-optimization problem in scalar and matrix form. For simplicity, we pose the problem in scalar form, which will give insight on the type of optimization problem we are solving.[1]

[1] *Note*: The numerical values for the inequality constraints on decision variables are given in Section 2.6

Posing the Optimization Problem in Scalar Form

$$(P_1) = \text{minimize } \ c_E N_{Eo} - c_Y N_Y = \nu^*$$

s.t.

$$\frac{dN_E}{dz} = -k_1^f \frac{N_E}{\overline{u}} + k_1^r \frac{N_Y N_H}{\overline{u}^2} - 2k_2 \frac{N_E}{\overline{u}} - k_8 \frac{N_E N_Y}{\overline{u}^2}, \qquad N_E(z=0) = N_{Eo}$$

$$\frac{dN_Y}{dz} = k_1^f \frac{N_E}{\overline{u}} - k_1^r \frac{N_Y N_H}{\overline{u}^2} - k_6 \frac{N_A N_Y}{\overline{u}^2} - k_8 \frac{N_E N_Y}{\overline{u}^2}, \qquad N_Y(z=0) = N_{Yo}$$

$$\frac{dN_H}{dz} = k_1^f \frac{N_E}{\overline{u}} - k_1^r \frac{N_Y N_H}{\overline{u}^2}, \qquad N_H(z=0) = 0$$

$$\frac{dN_P}{dz} = k_2 \frac{N_E}{\overline{u}}, \qquad N_P(z=0) = 0$$

$$\frac{dN_M}{dz} = k_2 \frac{N_E}{\overline{u}} + k_5^f \frac{N_L}{\overline{u}} - k_5^r \frac{N_M N_A}{\overline{u}^2} + k_8 \frac{N_E N_Y}{\overline{u}^2}, \qquad N_M(z=0) = 0$$

$$\frac{dN_L}{dz} = -k_5^f \frac{N_L}{\overline{u}} + k_5^r \frac{N_M N_A}{\overline{u}^2} + k_8 \frac{N_E N_Y}{\overline{u}^2}, \qquad N_L(z=0) = 0$$

$$\frac{dN_{Af}}{dz} = k_5^f \frac{N_L}{\overline{u}} - k_5^r \frac{N_M N_A}{\overline{u}^2} - k_6 \frac{N_A N_Y}{\overline{u}^2}, \qquad N_A(z=0) = 0$$

$$\frac{dN_{Bf}}{dz} = k_6 \frac{N_A N_Y}{\overline{u}^2}, \qquad N_B(z=0) = 0$$

$$\frac{dT}{dz} = \frac{-\Delta H_R R}{\overline{u}\rho C_p} + \frac{1}{\rho C_p}\frac{dP}{dz} + \frac{2U}{\overline{u}\rho C_p R}(T_{wall} - T), \qquad T(z=0) = T_o$$

$$\frac{dP}{dz} = \frac{\frac{1}{M}(\frac{0.092\mathrm{Re}^{-0.2}}{D})}{\frac{1}{MP} - \frac{P}{\alpha\rho^2\overline{u}^2 RT}}, \qquad P(z=0) = P_o$$

$$\mu = \sum_i \frac{\mu_i N_i}{N_i} \qquad C_p = \sum_i \frac{C_{pi} N_i}{N_i}$$

$$M = \sum_i \frac{M_i N_i}{N_i} \qquad k = \sum_i \frac{k_i N_i}{N_i}$$

$$\rho = \frac{PM}{RT} \qquad \overline{u} = \frac{RT}{P}(\sum_i N_i)$$

$$Re = \frac{\rho \overline{u} D}{\mu} \qquad k_z^{f \text{ or } r} = k_{z,o} e^{-\frac{E_z}{R_z T}}$$

$$\mu_i(T) = \frac{A_i T^{B_i}}{1 + \frac{C_i}{T} + \frac{D_i}{T^2}}$$

$$T_{o,min} \le T_o \le T_{o,max}$$

$$T_{wall,min} \le T_{wall} \le T_{wall,max}$$

$$P_{o,min} \le P_o \le P_{o,max}$$

$$n_{Eo,min} \le n_{Eo} \le n_{Eo,max}$$

$$L_{min} \le L \le L_{max}$$

$$L, T_o, T_{wall}, P_o, n_{Eo} \in \mathbb{R}$$
$$\forall i = E, Y, H, P, M, L, A, B, I$$
$$\forall z = 1, 2, 5, 6, 8$$

Type of Optimization Problem

Formalizing this problem in scalar form makes it convenient for us to write the general form of this problem. This optimization problem can be written as:

$$NLP_1 = min \quad f(x)$$

$$x \in \mathbb{R}^n$$

$$\text{s.t. } g(x) \leq 0$$

$$h(x) = 0$$

$$f : \mathbb{R}^n \to \mathbb{R}$$

$$g : \mathbb{R}^n \to \mathbb{R}^p, \quad p \leq n$$

$$h : \mathbb{R}^n \to \mathbb{R}^m, \quad m \leq n$$

$$f, g, h \in C^2$$

From this general form, it is obvious that the optimization problem is a nonlinear programming problem (NLP).

2.6 Justification of Decision Variables and Constraints

We can select the inlet feed conditions (n_I, n_{Ei}, n_{Yi}, P_o, and T_o) and tube conditions (D, L, and T_{wall}). However, we assume in this study that the inner diameter of the reactor is 0.1 m, which is approximately the inner diameter of a 4 inch schedule 80 stainless steel pipe. Furthermore, we assume that the inlet inert and ethylene feed conditions are 30% of the total feed by mole and 1 mol/s, respectively. Finally, we also need the single tubular reactor to fit in a 100 m by 1 m confined area. The remaining decision variables are feed temperature, constant wall temperature, feed pressure, tube length, and ethane molar feed. The constraints on each of the remaining decision variables are discussed below.

Feed Temperature

The temperature within the tube may not exceed 1323.15 K, which is 50 K below the highest operating temperature for standard alloys of stainless steel [25]. By the Arrhenius equation, a low temperature results in a very low reaction rate. Temperatures as low as 573.15 K result in almost no reactions taking place. Therefore, the bounds on the feed temperature are:

$$573.15 \text{ K} \leq T_o \leq 1323.15 \text{ K} \tag{2.5}$$

Constant Wall Temperature

We can use the same reasoning for the wall temperature constraint. Therefore, the bounds on the constant wall temperature are:

$$573.15 \text{ K} \leq T_{wall} \leq 1323.15 \text{ K} \tag{2.6}$$

Feed Pressure

The fact that the gas must be able to get to the end of the pipe constrains the inlet pressure. The pressure drop, which is found by integrating $\frac{dP}{dz}$ across the length of the pipe, must be at least 1 atm less than the inlet pressure so that the gas at the end is not stagnant. The pressure must also be below the burst pressure of the steel tube. We fit a logarithmic curve to the burst pressure for a 4 inch schedule 80 stainless steel pipe as a function of temperature [25]. The burst pressure at 1323.15 K is 73 atm. Therefore, the bounds on feed pressure are:

$$1 \text{ atm} \leq P_o \leq 73 \text{ atm} \tag{2.7}$$

Tube Length

The length of the tube must fit within the 100 m by 1 m area set by our project manager. Furtheremore, the length of the tube must not be too short where the V/A ratio does not favor heat transfer. Therefore, the minimum length is set equal to 1 m. The bounds on tube length are thus:

$$1 \text{ m} \leq L \leq 100 \text{ m} \tag{2.8}$$

Ethane Molar Feed

The ethane molar feed cannot be less than zero to be physically meaningful. However, test simulations indicate that an initial velocity greater than 750 m/s (corresponding to $n_{Eo} = 500$ mol/s) puts the process at risk of a velocity runoff along the tube. Therefore, the bounds on the ethane molar feed are:

$$0 \text{ mol/s} \leq n_{Eo} \leq 500 \text{ mol/s} \tag{2.9}$$

2.7 Proof of Feasibility and Optimality

We use the Weierstrass theorem to prove feasibility and optimality of this cost-optimization problem. The Weierstrass theorem states [26]:

> "*Let $f : \Omega \to \mathbb{R}$ be a continuous function, where $\Omega \subset \mathbb{R}^n$ is a compact set. Then, there exists $x_0 \in \Omega$ such that $f(x_0) \leq f(x)$ for all $x \in \Omega$. In other words, f achieves its minimum on Ω.*"

To use this theorem, we will first define the objective function. Next, we will show the set is compact, and the function outputs a scalar real-value. Finally, we will show the function is continuous. If we show each of these hold, then there exists a feasible and optimal solution to this cost-optimization problem.

Step 1: Define $f(x)$, x, and Ω from the problem statement

The scalar form of the problem statement suggests that $f(x)$, x, and Ω can be defined as:

$$f : \mathbb{R}^5 \to \mathbb{R} \tag{2.10}$$

$$x^T = [n_{Eo} \;\; T_o \;\; P_o \;\; T_{wall} \;\; L] \subset \mathbb{R}^5 \tag{2.11}$$

$$\Omega \subset \mathbb{R}^5 \tag{2.12}$$

Step 2: Show Ω is a compact set

From our definition of Ω in Step 1 and the constraints set on our decision variables, it is evident that Ω is both closed and bounded. Furthermore, $\Omega \subset \mathbb{R}^5$. Therefore, by definition, Ω is a compact set.

Step 3: Show $f : \Omega \to \mathbb{R}$

From our definition of f in Step 1, it is evident that f outputs a real-number scalar value from an input $\mathbf{x} \in \Omega$ (i.e. f is a functional on $\mathbf{x} \in \Omega$). Therefore, $f : \Omega \to \mathbb{R}$

Step 4: Show f is a continuous function

We define f as a linear function of N_Y and N_{Eo}. Therefore, if N_Y and N_{Eo} are continuous, f will also be continuous.

1. $N_{Eo} = \frac{4n_{Eo}}{\pi D^2}$. Since n_{Eo} is an independent variable and N_{Eo} is linearly dependent on n_{Eo}, N_{Eo} is continuous.

2. N_Y is at the very least C^1, as $\frac{dN_Y}{dz} = k_1^f \frac{N_E}{\overline{u}} - k_1^r \frac{N_Y N_H}{\overline{u}^2} - k_6 \frac{N_A N_Y}{\overline{u}^2} - k_8 \frac{N_E N_Y}{\overline{u}^2}$. Since N_Y is differentiable, it must be continuous.

Since N_Y and N_{Eo} are continuous, and f is a linear function of N_Y and N_{Eo}, f is also continuous.

Since each of the conditions of the Weierstrass theorem are met, there exists $x_0 \in \Omega$ such that $f(x_0) \leq f(x)$ for all $x \in \Omega$. In other words, there exists a feasible and optimal solution to the cost-optimization problem.

2.8 Algorithms Used in This Study

Due to the ordinary differential equation constraints, we apply an ordinary differential equation solver with the optimization algorithm. Our optimization algorithm, we use a trust-region algorith to enforce descent of the objective function. To solve the ordinary differential equation solver, we use the Runge-Kutta-Fehlberg method. The solution to the optimization problem by applying these algorithms is shown in the next section. A detailed explanation of each of these algorithms is shown in Appendix B.

Results

3.1 Computer Program Simulation

To solve our cost-optimization problem, we use MATLAB programming language (Natick, MA). There are five decision variables (T_o, T_{wall}, P_o, L, and n_{Eo}), ten dynamic equality constraints (N_E, N_Y, N_H, N_P, N_M, N_L, N_A, N_B, T, and P), ten initial condition constraints (N_{Eo}, N_{Yo}, N_{Ho}, N_{Po}, N_{Mo}, N_{Lo}, N_{Ao}, N_{Bo}, T_o, and P_o), twenty three algebraic equality constraints (μ, C_p, M, k, ρ, $\overline{u}$, Re, k_1^f, k_2, k_5^f, k_6, k_8, k_1^r, k_5^r, μ_E, μ_Y, μ_H, μ_P, μ_M, μ_L, μ_A, μ_B, and μ_I), and ten inequality constraints (two for each of the five decision variables).

Our algorithm couples an ordinary differential equation solver with a convex optimization solver. A detailed version of the code is shown in Appendix C. This optimization problem takes approximately 3.8 seconds to solve.

3.2 Solution to Problem Statement

The optimal solution to the cost-optimization problem is shown below (Table 3.1).

TABLE 3.1: Optimal Solution to the Cost-Optimization Problem

Decision Variable	Optimal Solution to Cost-Optimization Problem
T_o	1323.15 K
P_o	4.3 atm
L	100 m
T_{wall}	1323.15 K
n_{Eo}	500 mol/s

The optimal value, $f(\mathbf{x}^*)$, is equal to $\$3.60/s$, which is equivalent to over $\$112,000,000$ per year. Therefore, our original assumption that the additional capital costs to retrofit the furnace will be negligible compared to the profit is valid.
Previous design engineers at our company ran at the following operating conditions:

1. $n_{Eo} = 99$ mol/s
2. $n_{Yo} = 1$ mol/s
3. Mole fraction of inert in inlet stream = 0.4
4. $D = 0.1$ m
5. $L = 85$ m
6. $T_o = 1123.15$ K
7. $T_{wall} = 1073.15$ K
8. $P_o = 12$ atm

At these conditions, our company was profiting $\$22,000,000$ per year, or $\$0.69/s$. Our optimal value is significantly greater than previous operating conditions, as expected.

Most of our optimal solutions lie on the boundary of its set (T_{wall}, T_o, n_{Eo}, and L), while P_o does not. T^*_{wall}, T^*_o, L^*, and n^*_{Eo} are equal to $T_{wall,max}$, $T_{o,max}$, L_{max}, and $n_{Eo,max}$, respectively. When we each of these constraints, there is greater profit. However, this is extremely risky, as there is a great chance for the pipe to burst, or the pressure and velocity to runoff. Therefore, we recommend the safer option that is still extremely profitable − running at x^*.
We created 2-dimensional and 3-dimensional plots to validate our results (Figures 3.1, 3.2, 3.3, and 3.4). By the first order necessary condition (FONC), we require the partial derivative of the objective function with respect to each decision variable to equal zero, unless the optimal value for the decision variable is on the boundary of its set. In our case, the solution was on the boundary of the set, so FONC is satisfied if:

$$d^T \bigtriangledown f(x^*) \geq 0 \tag{3.1}$$

where d is any feasible direction at x^*. Figures 3.1, 3.2, 3.3, and 3.4 show that this holds true for each case examined. This suggests our optimal solution is indeed valid.

First, we input T^*_{wall}, n^*_{Eo}, T^*_o, and P^*_o with varying L. Therefore, the cost function became a function of length (Figure 3.1). Holding everything but L constant, the only feasible direction is to decrease L. When doing so, the profit decreases, which increases the objective function, making $d^T \bigtriangledown f(x^*) \geq 0$ hold.

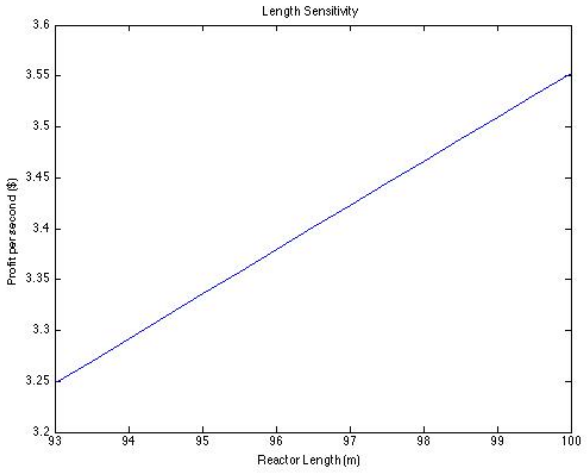

FIGURE 3.1: The cost function as a function of length when all other decision variables are held constant.

Next, we input T^*_{wall}, $L*$, T^*_o, and P^*_o with varying n^*_{Eo}. Therefore, the cost function became a function of ethane feed (Figure 3.2). Holding everything but n_{Eo} constant, the only feasible direction is to decrease n_{Eo}. When doing so, the profit decreases, which increases the objective function, making $d^T \bigtriangledown f(x^*) \geq 0$ hold.

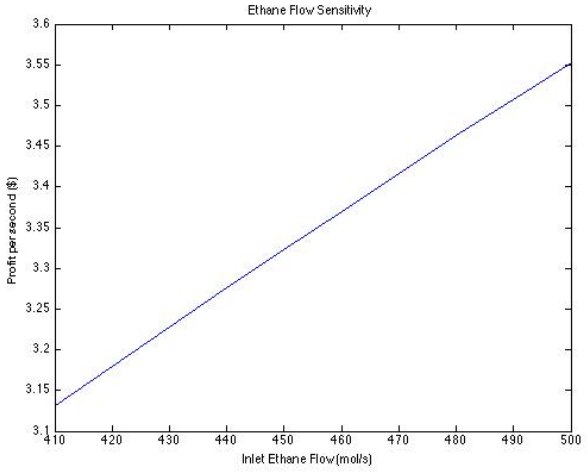

FIGURE 3.2: The cost function as a function of ethane feed when all other decision variables are held constant.

Next, we input T^*_{wall}, $L*$, T^*_o, and n^*_{Eo} with varying P^*_o. Therefore, the cost function became a function of inlet pressure (Figure 3.3). Holding everything but P_o constant, both increasing and decreasing P_o. When doing so, the profit decreases, which increases the objective function, making $d^T \bigtriangledown f(x^*) \geq 0$ hold.

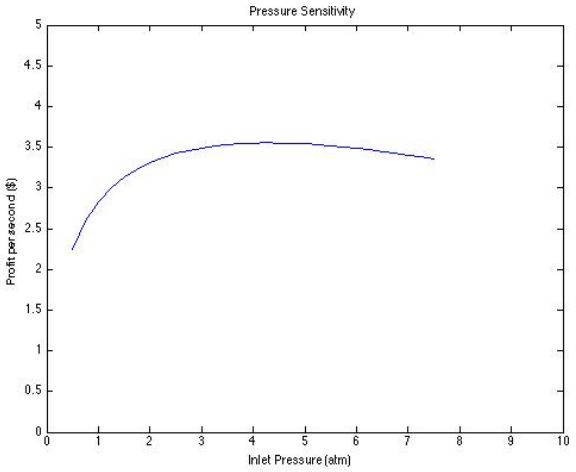

FIGURE 3.3: The cost function as a function of inlet pressure when all other decision variables are held constant.

Finally, we created a 3-dimensional plot where the cost function is a function of T_{wall} and T_o for constant $n_{Eo} = n^*_{Eo}$, $P_o = P^*_o$, and $L = L^*$ (Figure 3.2). From this 3-dimensional plot, it is evident that the profit function decreases with a decrease in wall temperature or inlet temperature, making $d^T \bigtriangledown f(x^*) \geq 0$ hold.

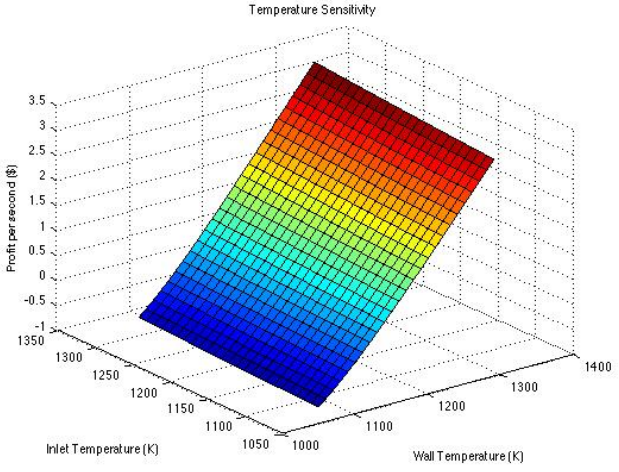

FIGURE 3.4: Cost function as a function of T_{wall} and T_o.

In the next section, we show that perturbing our parameters results in little change in our optimal solution. This gives us confidence in the methodology of our study.

3.3 Sensitivity Analysis

To determine how strongly the optimal profit depends on the parameters defining the system, we varied select parameters and observed the affect on the output. The parameters we varied include the viscosity of the stream, the thermal conductivity of the stream, and the specific heat of the stream. Additionally, we varied physical properties of the tubular reactor, such as the diameter of the tube. The results of the sensitivity analysis are shown below (Table 3.2).

TABLE 3.2: Sensitivity Analysis on Cost-Optimization Problem

Parameter	Δ Parameter (%)	Δ Profit (%)
μ	-10	$+13$
μ	-20	$+20$
μ	$+10$	-11
μ	$+20$	-20
k	-10	-17
k	-20	-32
k	$+10$	$+18$
k	$+20$	$+36$
C_p	-10	-10
C_p	-20	-19
C_p	$+10$	$+10$
C_p	$+20$	$+19$
D	$+100$	-64
D	-50	$+61$

From these perturbations of parameters, it is evident that the profit is slightly sensitive to very large changes in parameters such as viscosity, specific heat, and thermal conductivity. The output was very sensitive to large changes in the diameter of the tube, as these specifications alter the velocity and thus the pressure drop greatly. We can qualitatively explain how the perturbations of parameters resulted in the increase or decrease in profit. For example, as the viscosity increases, the Reynolds number decreases, and the pressure drop increases, making the profit decrease. Furthermore, as the thermal conductivity increases, the temperature of the stream approaches the temperature of

the wall faster, making the rate of reaction increase and thus a greater profit. Finally, as the diameter increases with constant n_{Eo}, N_{Eo} decreases, making the production of ethylene decrease, giving a lower profit.

Conclusions/Future Work

To solve a cost-optimization problem for the thermal cracking process of ethane to ethylene, we formulated a constrained, nonlinear programming problem. We selected the length of the tube, the inlet feed temperature, the constant wall temperature, the feed pressure, and the ethane molar feed as decision variables to optimize profit. The optimal profit value is $\$3.60/s$, which is equivalent to over $\$112,00,000$ per year, when the feed temperature, constant wall temperature, feed pressure, tube length, and ethane molar feed are 1323.15 K, 1323.15 K, 4.29 atm, 100 m, and 500 mol/s, respectively. This profit is much greater than the previous conditions at our company, where profited less than $\$22,00,000$ per year.

In the future, numerous enhancements can be made for our model. For example, we assume that the only costs were the ethane feedstock and the ethylene product. However, other factors would be considered in a future analysis of this process, such as the cost of separating ethylene from the reactor effluent, the cost of heating the reactor, and the cost of the tube itself. With more information about the separation process, we would also be able to examine the possibility of a recycle stream and include its flowrate and composition as decision variables in our optimization. Beyond these considerations, we could relax the definitions on some decision variables, and potentially optimize the feed concentrations of inerts and ethylene, and the tube diameter, in addition to our current five decision variables.

Appendix A

Plug Flow Reactor Supplementary Information

To model the design equation of a plug flow reactor, it is necessary to use a mole balance on the control volume shown in Figure A.1 and take the limit as $\Delta z \to 0$ [1]. The resulting design equation is:

$$\overline{u}\frac{dC_A}{dz} = R_A \tag{A.1}$$

where $\overline{u}$ is the velocity at a position z along the reactor, C_A is the concentration of species A, and R_a is the rate of reaction [1]. Typically, the stream flow rate is high enough for the bulk term to dominate in the molar flux equation:

$$N_A = \overline{u}C_A + \nabla \cdot C_A + (\text{eddy diffusion term}) \tag{A.2}$$

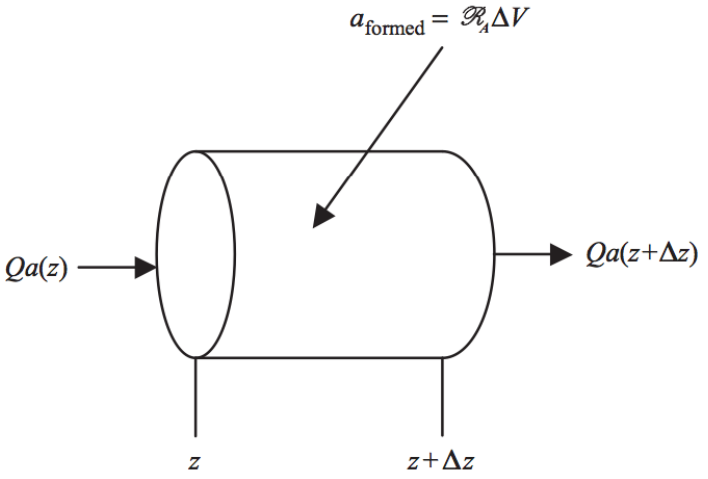

FIGURE A.1: Mole balance on plug flow reactor for a small Δz [1]

so that $\overline{u}C_A = N_A$, where N_A is the molar flux of species A. Therefore, the total molar rate of species A, n_A is:

$$n_A = A_{pfr} N_A \tag{A.3}$$

where A_{pfr} is the cross-sectional area of the plug flow reactor.

The rate constant of the reaction, k, is highly dependent on the temperature based on the Arrhenius equation ($k = k_o e^{-\frac{E}{RT}}$). Therefore, it is necessary to find the temperature along the reactor for non-isothermal cases. An energy balance on a small control volume along the reactor allows us to model the temperature profile (Figure A.2) [1].

By using an energy balance on the control volume shown in Figure A.2, and taking the limit as $\Delta z \to 0$, the temperature change along the plug flow reactor is [1]:

$$\frac{dT}{dz} = \frac{-\Delta H_R R}{\overline{u}\rho C_p} + \frac{1}{\rho C_p}\frac{dP}{dz} + \frac{2U}{\overline{u}\rho C_p R}(T_{ext} - T) \tag{A.4}$$

where ΔH_R is the enthalpy of reaction, ρ is the average density of the stream at location z, $\frac{dP}{dz}$ is the change in pressure along the reactor, C_p is the average specific heat, U is the overall heat transfer coefficient, R is the radius of the tube, and T_{ext} is the wall temperature [1]. The pressure drop along the reactor during turbulent flow is [1]:

$$\frac{dP}{dz} = -\frac{0.079\rho\overline{u}^2}{Re^{1/4}R} \tag{A.5}$$

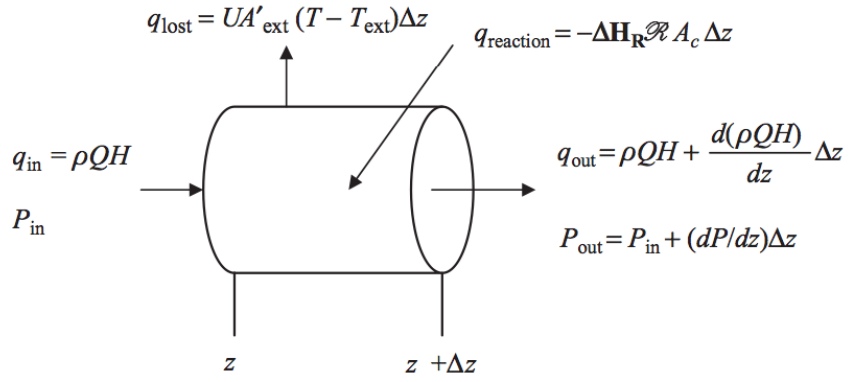

FIGURE A.2: Energy balance on plug flow reactor for a small Δz [1]

Appendix B

Algorithms Used in This Study

Optimization Algorithm

To enforce the descent of an objective function at every iteration in an algorithm, two general methods are typically used: line searches and trust-regions. Line search algorithms first choose a search direction, and then the distance along this direction. Trust-regions, on the other hand, select the maximum distance to go along in an iteration, followed by the direction (Figure B.1) [27]. In this study, we use the "fmincon" MATLAB function to optimize the problem of interest, which uses a trust-region algorithm.

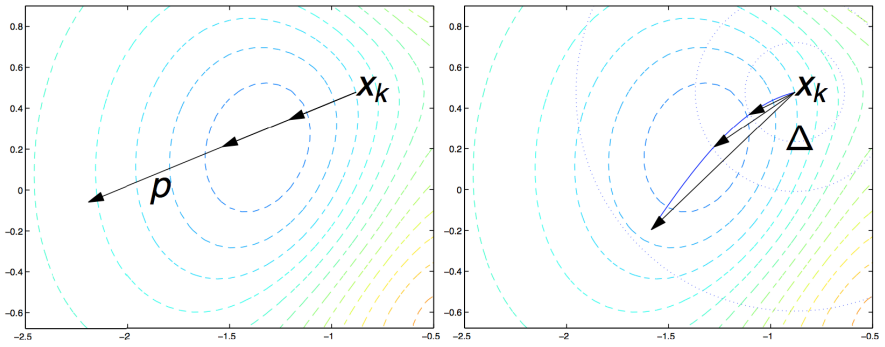

FIGURE B.1: The difference between line-search and trust-region algorithms are depicted above. In the figure to the left, a line-search algorithm is applied, as the search direction is first selected, followed by the distance along this direction. In the figure to the right, a trust-region algorithm is applied, as the maximum distance to go along is selected first, followed by the direction [27].

To minimize the objective function $f(x)$, it is necessary to find the next point x_{i+1} that gives a smaller $f(x)$ until $f(x)$ no longer decreases. To do so, $f(x)$ can be approximated by its Taylor series expansion around x_i in a neighborhood ϵ around x_i. The next step size s_i can be approximated by solving the optimization problem [28]:

$$\begin{aligned} &min \;\; q_i(s) \\ &s.t. \;\; ||x|| \leq \epsilon \end{aligned} \tag{B.1}$$

$$q_i(s) = \mathbf{g}^T s + \tfrac{1}{2} s^T \mathbf{H} s$$

where $\mathbf{g}$ and $\mathbf{H}$ are the gradient and the Hessian of $f(x)$ at x_i, respectively [28]. The optimal step size, x^* of this constrained optimization problem is the solution to:

$$(\mathbf{H} + \lambda \mathbf{I}) x^* = -\mathbf{g} \tag{B.2}$$

for $\lambda \geq 0$ and a positive semi-definite matrix $\mathbf{H} + \lambda \mathbf{I}$. Adapted trust-region sizes are typically applied for algorithms to compare the predicted and actual reduction of the objective function [27]. The reduction ratio ρ dictates the modifications of the trust-region step size, where the reduction ratio is:

$$\rho = \frac{f(x_i) - f(x_i + s_i)}{q_i(0) - q_i(s_i)} \tag{B.3}$$

If the reduction ratio is greater than $\frac{3}{4}$, the trust-region step size is increased during the next iteration. If the reduction ratio is less than $\frac{1}{4}$, the trust-region step size is decreased during the next iteration. It is necessary for the reduction ratio to not be too small in order for the step s to be used on an iteration [27]. In our study, the objective function is dependent on the integration of ordinary differential equations. Therefore, we need to use an ordinary differential equation solver.

Ordinary Differential Equation Solver

By formally posing the problem statement, it is clear that ordinary differential equations are existent in the constraint set. Therefore, we use an ordinary differential equation solver to numerically solve these ordinary differential equations. We use the Runge-Kutta-Fehlberg method in this study to numerically solve the ordinary differential equations [29, 30].

The Runge-Kutta-Fehlberg method checks and compares two different approximations for the numerical solution of an ordinary differential equation to determine if the correct step size is used. If the two approximations are nearly equation, the step size is used. However, if the two approximations are not nearly equation, the step size is decreased. The calculation of the step size h requires the calculation of k_1 through k_6:

$$k_1 = h f(t_k, y_k) \tag{B.4}$$

$$k_2 = h f(t_k + \frac{1}{4} h, y_k + \frac{1}{4} k_1) \tag{B.5}$$

$$k_3 = h f(t_k + \frac{3}{8} h, y_k + \frac{3}{32} k_1 + \frac{9}{32} k_2) \tag{B.6}$$

$$k_4 = hf(t_k + \frac{12}{13}h, y_k + \frac{1932}{2197}k_1 - \frac{7200}{2197}k_2 + \frac{7296}{2197}k_3) \tag{B.7}$$

$$k_5 = hf(t_k + h, y_k + \frac{439}{216}k_1 - 8k_2 + \frac{3680}{513}k_3 - \frac{845}{4104}k_4) \tag{B.8}$$

$$k_6 = hf(t_k + \frac{1}{2}h, y_k - \frac{8}{27}k_1 + 2k_2 - \frac{3544}{2565}k_3 + \frac{1859}{4104}k_4 - \frac{11}{40}k_5) \tag{B.9}$$

The fourth order y_{k+1} and fifth order z_{k+1} approximations of the initial value problem are then calculated by Equations B.10 and B.11, respectively:

$$y_{k+1} = y_k + \frac{25}{216}k_1 + \frac{1408}{2565}k_3 + \frac{2197}{4101}k_4 - \frac{1}{5}k_5 \tag{B.10}$$

$$z_{k+1} = y_k + \frac{16}{135}k_1 + \frac{6656}{12,825}k_3 + \frac{28,561}{56,430}k_4 - \frac{9}{50}k_5 + \frac{2}{55}k_6 \tag{B.11}$$

The optimal step size sh is then determined by calculating s:

$$s = \left(\frac{\epsilon h}{2|z_{k+1} - y_{k+1}|}\right)^{\frac{1}{4}} \tag{B.12}$$

where ϵ is the tolerance selected. We apply this ordinary differential equation solver along the length of the tube, and we subsequently apply the trust-region algorithm to minimize the objective function.

Appendix C

MATLAB Code

```
% Throughout this code, there will be matrices referring to the components
% in a consistent order. This order is: [E Y H P M L A B I].


function OptimalReactor
format long;          % Display variables in double precision
clear all;            % Clear all existing variables
close all;            % Close open figure windows
clc;                  % Clear the command window

% Inlet conditions that are fixed:

nYo = 1;          % Inlet ethylene molar flow per second
yI = 0.3;         % Inlet mole fraction of steam
R = 8.314;        % Gas constant - J/mol/K
R2 = R/4184;      % Gas constant - kcal/mol/K
d = 0.1;          % Tube diameter - m
Ac = pi*d^2/4;    % Tube area - m^2

% Molecular weights of the speceies, in kg/mol:

M = [30.07 28.054 2.016 44.096 16.042 42.08 26.037 54.092 18.016]./1000;

% Coefficients for heat capacity in J/mol/K:

%           A          B       C       D       E
CP      = [44.256     84.737  872.24  67.130  2430.4   %Ethane
           33.380     94.790  1596    55.100  740.8    %Ethylene
           27.617     9.560   2466    3.760   567.6    %Hydrogen
           59.474     12.661  844.31  86.165  2482.7   %Propane
           33.298     79.933  2086.9  41.602  991.96   %Methane
           43.852     15.060  1398.8  74.754  616.46   %Propylene
```

```
          36.921    31.793  678.05  33.430  3036.6   %Acetylene
          50.950    17.050  1532.4  13.370  685.6    %Butadiene
          33.363    26.790  2610.5  8.896   1169];   %Water

% Heats of formation in J/mol:

H = [-8.382e4
    5.251e4
    0
    -1.0468e5
    -7.452e4
    2.023e4
    2.282e5
    1.0924e5
    -2.41818e5];

% Stoichoimetric coefficient matrix:

Mv = [-1 1 1 0 0 0 0 0 0
       -2 0 0 1 1 0 0 0 0
       0 0 0 0 1 -1 1 0 0
       0 -1 0 0 0 0 -1 1 0
       -1 -1 0 0 1 1 0 0 0];

% The actual optimization:

% Initial guess:

         %To     %Tw    %Po    %nEo %L
beta0 = [13 13 10 .75 8];

% Minimum constraints on decision variables:

min = [5.7315 5.7315 1 0 1];

% Maximum constraints:

max = [13.2315 13.2315 73 5 10];

% Maximum number of iterations

options=optimset(MaxFunEvals,500,Algorithm,active-set,TolFun,1e-8);

%[Best] = fmincon(@ReactorOutput,beta0,[],[],[],[],min,max,[],options);

% revenue = -ReactorOutput(Best)*3600*24*365
%
% Tobest = 100*Best(1)
```

```
% Twbest = 100*Best(2)
% Pobest = Best(3)
% nEobest = 100*Best(4)
% Lbest = 10*Best(5)


function profit = ReactorOutput(In)
    To = 100*In(1);
    Tw = 100*In(2);
    Po = In(3)*101325;
    nEo = 100*In(4);
    L = 10*In(5);

    % Must find the enthalphy of each component at the inlet by integrating
    % Cp from 298.15 K to the inlet temp.

    Tref = 298.15;

    for i = 1:1:9
        A = CP(i,1);
        B = CP(i,2);
        C = CP(i,3);
        D = CP(i,4);
        E = CP(i,5);
        CpInt(i,1) = A*To + B*C/coth(C/To) - D*E/tanh(E/To) - ...
        (A*Tref + B*C/coth(C/Tref) - D*E/tanh(E/Tref));
    end

    Hform = H + CpInt;

    Hrxn = Mv*Hform;

    % Initial specifications; inlet molar fluxes, P, and T. Stored in a
    % vector of initial guesses, Wo.

    NIo = yI*(nEo+nYo)/(1-yI)/Ac;  % Inlet molar flux of steam
    NEo = nEo/Ac;
    NYo = nYo/Ac;

    Wo = [NEo NYo 0 0 0 0 0 0 NIo Po To];

    % Inlet mass flux

    G = Wo(1:9)*M;

    % Coefficient for pressure drop calculations
    Pcoeff = 0.092*(4/pi)^-0.2/d^1.2*G^0.2;
```

```
% Coefficient for temperature change calculations
Tcoeff = 0.092*G^0.8/d^1.2;

% Evaluation of the ODEs
[z,W] = ode45(@diffeqs,[0 L],Wo);

% Ethylene mass flow at the end of the reactor:
nYout = W(end,2)*Ac*M(2);

% Subroutine defining the ODEs:

function [flows] = diffeqs(z,W)

% Total flux at this point:
N = sum(W(1:9));

% Velocity at this point:
v = R*W(11)*N/W(10);

% Rate constants at this temperature:
[k1f k1r k2 k5f k5r k6 k8] = ks(W(11));

% Viscosity and thermal conductivity at this temperature:
[u kt] = mukt(W(11),W(1:9));

% Viscosity at the wall:
[uw ktw] = mukt(Tw,W(1:9));

% Heat capacity at this temperature:
Cp = Cpval(W(11),W(1:9));

% Rate vector at this point:
Rates = [k1f*W(1)/v - k1r*Po/W(10)*W(2)*W(3)/v^2
         k2*(W(1)/v)
         k5f*W(6)/v - k5r*Po/W(10)*W(7)*W(5)/v^2
         k6*W(7)*W(2)/v^2
         k8*W(2)*W(1)/v^2];

% Flux ODEs:

dNE = (k1r*Po/W(10)*W(2)*W(3) - W(1)*(k8*W(2) + k1f*v + 2*k2))/v^2;
dNY = (k1f*v*W(1)-W(2)*(k1r*Po/W(10)*W(3)+k6*W(7)+k8*W(1)))/v^2;
dNH = (k1f*v*W(1) - k1r*Po/W(10)*W(2)*W(3))/v^2;
dNP = (k2*W(1))/v^2;
dNM = (k2*W(1) + k5f*v*W(6)-k5r*Po/W(10)*W(5)*W(7)+k8*W(1)*W(2))/v^2;
dNL = (k5r*Po/W(10)*W(5)*W(7) - k5f*v*W(6) + k8*W(1)*W(2))/v^2;
dNA = (k5f*v*W(6) - W(7)*(k5r*Po/W(10)*W(5) + k6*W(2)))/v^2;
dNB = (k6*W(2)*W(7))/v^2;
```

```
% P and T ODEs:
dP = Pcoeff*u^0.2/(M*W(1:9));
dT = (Cp*G)^-1*(-Hrxn*Rates + dP*v + ...
    Tcoeff*kt^(2/3)*Cp^(1/3)/uw^0.14/u^(0.327)*(Tw-W(11)));
flows = [dNE dNY dNH dNP dNM dNL dNA dNB 0 dP dT];
end

% Rate constants at a given T:

function [k1f k1r k2 k5f k5r k6 k8] = ks(Temp)

k1f = 4.652e13*exp(-65.20/R2/Temp);
k1r = k1f*exp((134.91 - 0.0895*Temp)*1000/R/Temp)/1000/(Po/R/Temp);
k2 = 3.850e11*exp(-65.25/R2/Temp)/1000;
k5f = 9.814e8*exp(-36.92/R2/Temp);
k5r = k5f*exp((124.79 - 0.0806*Temp)*1000/R/Temp)/1000/(Po/R/Temp);
k6 = 1.026e12*exp(-41.26/R2/Temp)/1000;
k8 = 7.083e13*exp(-60.43/R2/Temp)/1000;

end

% Viscosity and thermal conductivity at a given T and composition:

function [u kt] = mukt(Temp,N)


 % Thermal conductivity coefficients:

 K = [7.3869E-05 1.1689E+00 5.0073E+02 0
 8.6806E-06 1.4559E+00 2.9972E+02 -2.9403E+04
 2.6530E-03 7.4520E-01 1.2000E+01 0
-1.1200E+00 1.0972E-01 -9.8346E+03 -7.5358E+06
 8.3983E-06 1.4268E+00 -4.9654E+01 0
 4.4900E-05 1.2018E+00 4.2100E+02  0
 7.5782E-05 1.0327E+00 -3.6227E+01 3.1432E+04
-2.0890E+04 9.5930E-01 -9.3820E+10 0
 6.2041E-06 1.3973E+00 0 0];

% Viscosity coefficients:

V = [2.5906E-07 0.67988 98.902  0
2.0789E-06  0.4163  352.7   0
1.797E-07   0.685   -0.59   140
4.9054E-08  0.90125 0   0
5.2546E-07  0.59006 105.67  0
7.3919E-07  0.5423  263.73  0
1.2025E-06  0.4952  291.4   0
```

```
2.696E-07   0.6715  134.7   0
1.7096E-08  1.1146  0   0];

% Evaluated for each component:

for j = 1:1:9
    ui(j) = V(j,1)*Temp^V(j,2)/(1+V(j,3)/Temp+V(j,4)/Temp^2);
    ki(j) = K(j,1)*Temp^K(j,2)/(1+K(j,3)/Temp+K(j,4)/Temp^2);
end

% Total viscosity - mass weighted sum:

u = (N.*M)*ui/sum(N.*M);

% Total thermal conductivity - mass weighted sum:

kt = (N.*M)*ki/sum(N.*M);

end

% Heat capacity of the mixture at a given T and composition

function Cptot = Cpval(Temp,N)

for i = 1:9
    A = CP(i,1);
    B = CP(i,2);
    C = CP(i,3);
    D = CP(i,4);
    E = CP(i,5);
    Cp(i) = A + B*(C/Temp/sinh(C/Temp))^2 + D*(E/Temp/cosh(E/Temp))^2;
end

% Overall heat capacity - molar weighted sum:

Cptot = 1.2*Cp*(N/sum(N));

end

Ntot = W(:,1);

for i = 2:1:9
    Ntot = Ntot + W(:,i);
end

% Flow of ethylene leaving the reactor:

nYend = W(end,2)*Ac;
```

```
    % Negative profit per second:

    profit = -0.033*nYend + 0.0036*nEo;

end

% Best = [13.2315 13.2315 4.291385 5 10];

% % Pressure sensitivity:

% for n = 1:1:29
%     TestBest = Best;
%     p(n) = 0.25 + 0.25*n;
%     TestBest(3) = p(n);
%     Testp(n) = -ReactorOutput(TestBest);
% end

% figure(1)
% plot(p,Testp);
% axis([0 10 0 5]);
% xlabel(Inlet Pressure (atm));
% ylabel(Profit per second ($));
% title(Pressure Sensitivity);

% % Length sensitivity:
% for n = 1:1:15
%     TestBest = Best;
%     l(n) = 100.5 - 0.5*n;
%     TestBest(5) = 0.1*l(n);
%     Testl(n) = -ReactorOutput(TestBest);
% end
%
% figure(2)
% plot(l,Testl);
% xlabel(Reactor Length (m));
% ylabel(Profit per second ($));
% title(Length Sensitivity);
%
% % Ethane flow sensitivity
%
% for n = 1:10
%     TestBest = Best;
%     e(n) = 510 - 10*n;
%     TestBest(4) = 0.01*e(n);
%     Teste(n) = -ReactorOutput(TestBest);
% end
%
```

```
% figure(3)
% plot(e,Teste);
% xlabel(Inlet Ethane Flow (mol/s));
% ylabel(Profit per second ($));
% title(Ethane Flow Sensitivity);


% % Temperature sensitivity

% for n = 1:1:25
%     for o = 1:1:25
%         TestBest = Best;
%         tw(n) = 13.2315 - 0.1*n;
%         to(o) = 13.2315 - 0.1*o;
%         TestBest(1) = tw(n);
%         TestBest(2) = to(o);
%         Testt(n,o) = -ReactorOutput(TestBest);
%     end
% end

% figure(4)
% surf(100*tw,100*to,Testt);
% xlabel(Wall Temperature (K));
% ylabel(Inlet Temperature (K));
% zlabel(Profit per second ($));
% title(Temperature Sensitivity);



end

end
```

Bibliography

[1] B. E. Nauman. *Chemical Reactor Design, Optimization, and Scaleup*. Wiley, 2008.

[2] L.T. Biegler. *Nonlinear Programming: Concepts, Algorithms, and Applications to Chemical Processes*. Society for Industrial and Applied Mathematics and the Mathematical Optimization Society, 2010.

[3] K.M. Sundaram and G.F. Froment. Thermal cracking of ethane, propane and their mixtures. *Chemical Engineering Science*, 1977.

[4] S. Narayanan P.S. Van Damme and G.F. Froment. Thermal cracking of propane and propane-propylene mixtures: Pilot plant versus industrial data. *AICHE*, 1975.

[5] M.J. Shah. Computer control of ethylene production. *Industrial and Engineering Chemistry*, 1967.

[6] Dallas Kachan. The story of ethylene - now starring natural gas.

[7] UNEP Publications. Ethylene.

[8] Rainer Graefe. Vladimir grigorievich shukhov. URL http://www.shukhov.org/shukhov.html.

[9] Froment and Bischoff. *Chemical Reactor Analysis and Design*. Wiley, 1990.

[10] Knutzen and Katz. *Fluid Dynamics and Heat Transfer*. McGraw-Hill, 1958.

[11] Stainless steel pipes - dimensions and weights ansi/asme 36.19, . URL http://www.engineeringtoolbox.com/ansi-stainless-steel-pipes-d_247.html.

[12] B. Davis. Fall 2013: Homework 2.

[13] Chemical database temperature-dependent properties, . URL http://dippr.byu.edu/public/chemsearch.asp?Mode=Printout2&ChemID=2.

[14] Chemical database temperature-dependent properties, . URL http://dippr.byu.edu/public/chemsearch.asp?Mode=Printout2&ChemID=201.

[15] Chemical database temperature-dependent properties, . URL http://dippr.byu.edu/public/chemsearch.asp?Mode=Printout2&ChemID=3.

[16] Chemical database temperature-dependent properties, . URL http://dippr.byu.edu/public/chemsearch.asp?Mode=Printout2&ChemID=202.

[17] Chemical database temperature-dependent properties, . URL http://dippr.byu.edu/public/chemsearch.asp?Mode=Printout2&ChemID=401.

[18] Chemical database temperature-dependent properties, . URL http://dippr.byu.edu/public/chemsearch.asp?Mode=Printout2&ChemID=303.

[19] Chemical database temperature-dependent properties, . URL http://dippr.byu.edu/public/chemsearch.asp?Mode=Printout2&ChemID=902.

[20] Chemical database temperature-dependent properties, . URL http://dippr.byu.edu/public/chemsearch.asp?Mode=Printout2&ChemID=1.

[21] Chemical database temperature-dependent properties, . URL http://dippr.byu.edu/public/chemsearch.asp?Mode=Printout2&ChemID=1921.

[22] Mont belvieu ethane quotes, . URL http://www.cmegroup.com/trading/energy/petrochemicals/mont-belvieu-ethane-opis-5-decimals-swap_quotes_globex.html.

[23] Mont belvieu ethylene (pcw) financial futures, . URL http://www.cmegroup.com/trading/energy/petrochemicals/mont-belvieu-ethylene-pcw-financial-swap-futures_quotes_globex.html.

[24] D.W. Green R.H. Perry and J.O. Maloney. *Perry's Chemical Engineer's Handbook*. McGraw-Hill, 2003.

[25] Stainless steel pipes - pressure ratings, . URL http://www.engineeringtoolbox.com/stainless-steel-pipes-pressure-ratings-d_346.html.

[26] E. Chong and S. Zak. *An Introduction to Optimization*. John Wiley and Sons, 2001.

[27] Niclas Borlin. Nonlinear optimization: Trust-region methods.

[28] Jane Hung. Energy optimization of a diatomic system.

[29] Richard L. Burden and J. Douglas Faires. *Numerical Analysis*. Brooks-Cole, 2010.

[30] John H. Mathews. Runge-kutta-fehlberg method.